

Fuzzy-based variable impedance control of uncertain robot manipulator in flexible environment: A nonlinear force contact model-based approach

Ying Guo

Zhengzhou University

Jinzhu Peng (✉ jzpeng@zzu.edu.cn)

Zhengzhou University <https://orcid.org/0000-0002-2823-6571>

Shuai Ding

Zhengzhou University

Jing Liang

Zhengzhou University

Yaonan Wang

Hunan University

Research Article

Keywords: Variable impedance control, Flexible environment, Fuzzy logic system, Force contact model, Robotic system

Posted Date: September 27th, 2022

DOI: <https://doi.org/10.21203/rs.3.rs-2079422/v1>

License:  This work is licensed under a Creative Commons Attribution 4.0 International License.

[Read Full License](#)

Fuzzy-based variable impedance control of uncertain robot manipulator in flexible environment: A nonlinear force contact model-based approach

Ying Guo · Jinzhu Peng* · Shuai Ding ·
Jing Liang · Yaonan Wang

Received: date / Accepted: date

Abstract In this paper, a variable impedance control method is proposed for uncertain robotic systems based on a nonlinear force contact-based flexible environmental model. First, a nonlinear force contact model between the rigid manipulator and flexible environment is established to approximate more realistic interaction responses and to avoid excessive overshoot of the force that usually exists in the traditional spring-damping environmental model. Then, according to the force contact-based environmental model, a fuzzy-based adaptive variable impedance controller is designed to achieve position and force tracking of the manipulator, where the impedance parameters are adjusted online through the force and position feedback of the robotic system, and the fuzzy logic system (*FLS*) is used to compensate the uncertainties. The stability of adaptive variable impedance control is proved by Routh stability criterion and the boundness of all signals in the robotic system is proved by Lyapunov stability analysis. Finally, the effectiveness of the proposed method is verified by the simulation of a two-link manipulator.

Keywords Variable impedance control · Flexible environment · Fuzzy logic system · Force contact model · Robotic system

1 Introduction

Industrial robots have been widely applied to assembling, testing, polishing, welding, and other operations, which require direct interaction between the manipulator and the environment. The control of the interaction force of the manipulator is crucial in the process of performing tasks [1–3]. The application scenarios of robots are not limited to rigid environments, such as picking robots, cleaning robots, folding robots, and so on. Although the existing methods of manipulator force control research have been fruitful, including the interaction with rigid environment, the interaction force control between robot and flexible environment is still a challenging research direction due to the rapid development of the industrial level and the increasing demand for

Ying Guo · Jinzhu Peng · Shuai Ding · Jing Liang · Yaonan Wang
School of Electrical and Information Engineering, Zhengzhou University, Zhengzhou 450001, China
E-mail: jzpeng@zzu.edu.cn

Yaonan Wang
College of Electrical and Information Engineering, Hunan University, Changsha 410082, China
National Engineering Laboratory for Robot Visual Perception and Control, Hunan University, Changsha 410082, China

intelligence. So the compliance of the manipulator is strongly required to ensure the safety and stability of the robotic system in the process of performing tasks [4–6].

However, in most investigations, the contact environments of the robot are mainly rigid. In practical production and life, the majority of physical objects contacted with the manipulator are non-rigid [7]. It is worth noting that there are many modeling methods involving contact force with a flexible environment, where the contact force is usually modeled as a linear structure, such as a spring model or spring-damping mechanical system. Since many materials have nonlinear stiffness, the traditional linear structure has the limitations of only describing the linear contact force of objects and insufficient physical accuracy. Nonrigid environment usually has nonlinear characteristics, and the nonlinear model of the contact surface must be considered *et.al.* [8]. Luo *et.al.* [9] derived the nonlinear force model of a deformed object based on the Duffing equation, and proposed a unique method to simulate the force and deformation between rigid and elastic objects in complex contact. Omar *et.al.* [10] used a tapered spring method to simulate any linear and nonlinear behavior of soft tissue. Felix-Rendon *et.al.* [10] realized a non-rigid body deformation control scheme using finite element methods to simulate deformation dynamics. Selecting a sufficiently simple and powerful flexible environment model is the premise to solve the problem of compliant control in flexible environment.

At present, there are two mainstream compliance control methods: impedance control [11] and hybrid position/force control [12]. The impedance control takes motion and force into consideration, which selects different impedance parameters to adjust the relationship between the contact force and position [13] and has been widely used in contact force tracking [14–17]. Albu-Schaffer *et.al.* [18] improved the compliance of impedance controller in Cartesian space by local stiffness control. By adding integral terms to the traditional impedance model, Chen *et.al.* [19] eliminated tracking errors and improved the performance of the impedance controller. However, due to the friction, external disturbances, unknown joint velocities, and other uncertainties, the traditional impedance control is difficult to meet the requirements of control precision in the actual operation [20]. Since fuzzy logic and neural networks can deal with nonlinear and uncertain systems, and at the same time adapt to the human decision-making process and can learn, the method of combining them with traditional impedance control methods has been widely studied. To improve control precision of the uncertain manipulators, many researchers combine intelligent control with traditional impedance control [21–25]. He *et.al.* [26] designed a neural network-based adaptive impedance controller, which not only considered the system uncertainty in tracking control but also solved the input saturation. Subsequently, He *et.al.* [27] proposed an adaptive fuzzy neural network learning algorithm and adopted an impedance learning strategy to improve the interaction between the manipulator and the environment. In addition, Sun *et.al.* [28] proposed a composite learning impedance controller for robots with parameter uncertainties.

To realize contact force tracking of manipulators in flexible environment, the above compliance control method is also applied in flexible environment. Baptista *et.al.* [29] studied the application of a neural network impedance control scheme combining trajectory prediction algorithm with force error compensation. To enhance the robustness of the manipulator when interacting in a flexible environment, Jafari *et.al.* [30] and Wu *et.al.* [31] introduced an adaptive hybrid control method. The above methods have achieved good performance for flexible environment models. However, when the environments are uncertain or complicated, a controller with strong adaptive performance is required to meet the control accuracy of force.

Considering the poor adaptability of constant impedance control to the uncertainty of environmental stiffness, many researchers have studied variable impedance control [32–36]. Jung *et.al.* [32] proposed a new variable impedance control strategy, which minimized force error through the adaptive method. Variable impedance control can make up for the poor adaptability of constant impedance control, but the standard stability analysis is not appropriate for variable impedance

control. It is crucial to ensure the stable execution of variable impedance task. To prove the stability of the system, Kronander *et.al.* [37] proposed a state-independent stability constraint that related stiffness and its time derivative to damping. Duan *et.al.* [38] first proposed a control method based on tracking error to adjust impedance parameters online, and this method can compensate for environmental uncertainty. Roveda *et.al.* [39] proposed a sensorless model-based force control method, which improved the performance of force tracking by adjusting stiffness and damping parameters. Since the adaptive variable impedance control has strong adaptability to the unknown environment compared with the traditional control method, which has significance to study the force control of the robot in flexible environment.

In this paper, an adaptive variable impedance controller is applied to contact force control of the manipulator based on a nonlinear force contact model. The main contributions are as follows:

(1) Compared with the traditional spring-damping model, the nonlinear force contact model between rigid and elastic body is derived from Duffing equation, which can reflect the nonlinear characteristics of flexible objects and greatly reduce the overshoot of contact force in the initial contact stage. Based on the nonlinear force contact environmental model, the position-based adaptive variable impedance trajectory generator (*PBAVITG*) is designed to obtain the reference trajectory. The stability of *PBAVITG* is proved by Routh stability criterion, and the steady-state error of force tracking is also proved to be zero.

(2) Considering disturbance and uncertainty that exist in the practical robotic system and based on the environmental model, fuzzy-based adaptive variable impedance control (*FBAVIC*) is proposed to track the trajectory and interaction force, in which the impedance parameters are adjusted online by force feedback error, and *FLS* is used to compensate for the uncertainties. The boundedness of the signals are proved by Lyapunov theorem to ensure the stability of the controller.

2 Problem statement and Preliminaries

In this paper, \mathfrak{R} is defined as the real number set, \mathfrak{R}^n is defined as the n -dimensional real vector space, and $\mathfrak{R}^{n \times n}$ is defined as the $n \times n$ real matrix space. $I_{n \times n}$ is the $n \times n$ identity matrix.

2.1 Description of FLS

FLS can approximate any real continuous function over a compact set to arbitrary accuracy. According to the fuzzy control rules, the fuzzy inference engine performs fuzzy reasoning on the fuzzy input $x = (x_1, x_2, \dots, x_m)^T$ to solve the fuzzy relational equation and get the fuzzy output $y \in \mathfrak{R}$. The j th fuzzy rule is written as,

R^j : If x_1 is $A_1^{l_1}$ and ... x_m is $A_m^{l_m}$, Then y is B^j

where $l_i = 1, 2, \dots, q_i$ ($i = 1, 2, \dots, m$), q_i is the number of fuzzy set of the i th input x_i , $A_i^{l_i}$ and B^j ($j = \prod_{i=1}^m l_i$) are the fuzzy sets of input and output. The center of the fuzzy sets B^j ($j = 1, 2, \dots, p$) is defined as \bar{y}^j . By using product inference machine, single value fuzzier and center average fuzzier, the output of *FLS* is :

$$y(x) = \frac{\sum_{j=1}^p \bar{y}^j \left(\prod_{i=1}^m \mu_{A_i^{l_i}}(x_i) \right)}{\sum_{i=1}^{q_i} \left(\prod_{i=1}^m \mu_{A_i^{l_i}}(x_i) \right)} \quad (1)$$

where $\mu_{A_i^{l_i}}(x_i)$ is the membership function of x_i .

The fuzzy system basis function vector $\xi(x) = (\xi_1(x), \xi_2(x), \dots, \xi_p(x))^T$ can be introduced, Eq (1) can be rewritten as,

$$y(x) = \hat{\Theta}^T \xi(x) \quad (2)$$

where $\hat{\Theta} = [\bar{y}^1, \bar{y}^2, \dots, \bar{y}^p]^T$ is the parameter vector, and $\xi_j(x) = \frac{\prod_{i=1}^m \mu_{A_i^{l_i}}(x_i)}{\sum_{l_i=1}^{q_i} \left(\prod_{i=1}^m \mu_{A_i^{l_i}}(x_i) \right)}$.

In this paper, we use *FLS* to approximate the uncertain nonlinear function, yeild.

$$\Psi(x) = \Theta^{*T} \xi(x) + \varepsilon(x) \quad (3)$$

where Θ^* is ideal adptive adjustment parameter and $\varepsilon(x)$ is the minimum reconstruction error. Assuming exist a compact set $\Omega_{\Theta}^* = \{\Theta^* \in \mathbb{R}^p : \|\Theta^*\| \leq E_{\Theta}\}$ in which ideal parameters exist. The ideal parameter is expressed as,

$$\Theta^* = \arg \min_{\Theta^* \in \Omega_{\Theta}^*} \left\{ \sup |\Psi(x) - \hat{\Theta}^T \xi(x)| \right\} \quad (4)$$

2.2 Modeling of flexible environment

In this subsection, flexible objects made of isotropic elastic materials are studied. Duffing equation is one of the standard models for nonlinear systems under external forces, which essentially defines a nonlinear spring damp-restorer model [9]. A single-point contact with normal compression is showed in Fig. 1, where x_e indicates the original point of contact, which means the position before deformation, and x indicates the maximum deformation point. The normal contact force between rigid manipulator and flexible environment is defined as follows,

$$F_e = m(\omega_0^2 D + \frac{3\beta_0^2 \epsilon}{4} D^3) \quad (5)$$

where m is the mass of the rigid manipulator. ω_0 denotes the linear restoring force and $\beta_0^2 \epsilon$ is the parameters of nonlinear restoring term. $D = |x - x_e|$ is the deformation displacement. This model is sufficient to simulate complex behavior, and the contact forces of different flexible objects can be simulated by using different relevant parameters. Moreover, since a nonlinear recovery term is added to this model, which is used to represent the nonlinear recovery of the contact point of the flexible object, the model may reduce overshoot and oscillation when the manipulator is transforming from free space to contact space.

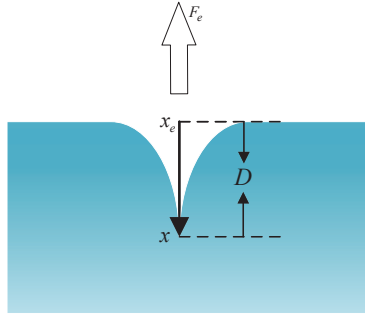


Fig. 1: Model of vertical contact force with flexible environment

It should be noted that the nonlinear force contact model has been presented in [9], however, no work has been reported to apply the model to the interaction compliance control for robots with flexible environment. Since this model has a nonlinear characteristic and is closer to the realistic interaction behavior in comparison to the traditional spring-damping model, the control process may be unstable, the traditional control methods may thus not show a good tracking performance. Therefore, it is necessary to design an improved compliance control method for the nonlinear force contact model.

2.3 Dynamic modeling and properties of robotic manipulator

The dynamic equation of n -link rigid robot obtained from Lagrange equation is expressed as follows,

$$M(q)\ddot{q} + C(q, \dot{q})\dot{q} + G(q) + \tau_d = \tau - \tau_e \quad (6)$$

where q , \dot{q} , and $\ddot{q} \in \mathfrak{R}^n$ are the joint position, velocity and acceleration vectors of the manipulator, respectively. $M(q)$ and $C(q, \dot{q}) \in \mathfrak{R}^{n \times n}$ are the inertia matrix and the centrifugal and Coriolis forces, respectively. $G(q)$, τ_d , τ and $\tau_e \in \mathfrak{R}^n$ denote the gravity vector, bounded unknown disturbances, torque input vector and interaction torque vector between manipulator and environment, respectively.

Considering the measurement error, environment, and payload factors, it is difficult to obtain the accurate physical parameters of the manipulator and the parameter matrix $M(q)$, $C(q, \dot{q})$ and $G(q)$ in the dynamic model. Therefore, we express the actual value $M(q)$, $C(q, \dot{q})$ and $G(q)$ as the nominal parts $M_0(q)$, $C_0(q, \dot{q})$ and $G_0(q)$ and the uncertain parts $\Delta M(q)$, $\Delta C(q, \dot{q})$ and $\Delta G(q)$, where $M(q) = M_0(q) + \Delta M(q)$, $C(q, \dot{q}) = C_0(q, \dot{q}) + \Delta C(q, \dot{q})$, $G(q) = G_0(q) + \Delta G(q)$. Then, the dynamic equation of the robot can be rewritten as follows,

$$M_0(q)\ddot{q} + C_0(q, \dot{q})\dot{q} + G_0(q) + Y(q, \dot{q}, \tau) + \tau_d = \tau - \tau_e \quad (7)$$

where $Y(q, \dot{q}, \tau) = \Delta M(q)\ddot{q} + \Delta C(q, \dot{q})\dot{q} + \Delta G(q) = \Delta M(q)[M^{-1}(q)(\tau - C(q, \dot{q})\dot{q} - G(q) - \tau_d - \tau_e)] + \Delta C(q, \dot{q})\dot{q} + \Delta G(q)$.

The following properties and assumption are required for the subsequent development.

Property 1 The inertia matrix $M(q)$ is positive definite, symmetric, and satisfies,

$$0 \leq M_m I_{n \times n} \leq M_0(q) \leq M_M I_{n \times n}, \forall q \in \mathfrak{R}^n \quad (8)$$

where M_m and M_M are positive constants.

Property 2 Matrix $\dot{M}(q) - 2C(q, \dot{q})$ is a skew symmetric matrix, i.e.

$$\zeta^T (\dot{M}_0(q) - 2C_0(q, \dot{q})) \zeta = 0, \forall \zeta \in \mathfrak{R}^n \quad (9)$$

Property 3 The norm $C(q, \dot{q})$ is bounded and satisfies,

$$\|C_0(q, \dot{q})\| \leq C_m \|\dot{q}\| \quad (10)$$

where C_m is a positive constant.

Assumption 1 The disturbance term is bounded, i.e

$$\|\tau_d\| \leq \tau_D \quad (11)$$

where τ_D is a positive constant.

The position and velocity vectors of the robot end-effector in Cartesian coordinate system are denoted by $X \in \mathfrak{R}^m$ and \dot{X} , respectively, and the relationship between Cartesian and joint coordinate system can be obtained as follows,

$$X = L(q), \dot{X} = J(q)\dot{q} \quad (12)$$

where $L(q)$ is the kinematic function of robot. $J(q) \in \mathfrak{R}^{m \times n}$ is the Jacobian matrix from joint coordinate system to Cartesian coordinate system.

The dynamic equation Eq (6) is converted to the Cartesian coordinate system and expressed as,

$$M_{0x}\ddot{X} + C_{0x}\dot{X} + G_{0x} + Y_x + F_{\tau_d} = F - F_e \quad (13)$$

where X , \dot{X} and \ddot{X} denote the position, velocity and acceleration vectors of the end-effector in Cartesian space, respectively, and $\ddot{X} = J\ddot{q} + \dot{J}\dot{q}$, $M_{0x} = J^{-T}M_0(q)J^{-1}$, $C_{0x} = J^{-T}C_0(q, \dot{q})J^{-1}$, $G_{0x} = J^{-T}G_0(q)$, $Y_x = J^{-T}Y(q, \dot{q}, \tau)$, $F_{\tau_d} = J^{-T}\tau_d$, $F = J^{-T}\tau$, $F_e = J^{-T}\tau_e$, and J is the shorthand of $J(q)$.

The objective of this paper is to design a trajectory generator and an adaptive variable impedance controller of end-effector in flexible environment, in which the trajectory generator can obtain a smooth reference trajectory to avoid excessive force overshoot when the manipulator transforms from free space to nonrigid contact space, and the controller can accurately track the reference trajectory and desired force of the manipulator with uncertainty.

3 Fuzzy-based variable impedance controller and stability analysis

In this section, the motion space of the robot is divided into flexible contact space and free space, and the contact force with the flexible environment is obtained by Duffing equation. According to the force contact model, the proposed *PBAVITG* is used to obtain the reference trajectory by adjusting the impedance parameters adaptively, and the *FBAVIC* is designed to realize the trajectory and desired force tracking of the end-effector. The *FLS* is used to approximate the uncertainty.

3.1 Position-based adaptive variable impedance trajectory generator

PBAVITG consists of an internal position control loop and an external force control loop, which can transform force feedback into position trajectory correction error and modify the reference trajectory input of the manipulator by adjusting impedance three parameters (inertia M_d , damping B_d and stiffness K_d) of the impedance controller. Then, the target impedance equation of robotic system is given as follows,

$$M_d\ddot{E} + B_d\dot{E} + K_dE = \Delta F \quad (14)$$

where $E = X_d - X$ is the error of position trajectory tracking, X_d , X respectively represent the expected position trajectory and actual position trajectory. \dot{E} and \ddot{E} represent velocity trajectory and acceleration trajectory tracking error, respectively, and $\Delta F = F_e - F_d$.

According to the contact force model Eq. (5) with the flexible object, it becomes,

$$\begin{cases} f_e = a_1(x - x_e) + a_2(x - x_e)^3 \\ \dot{f}_e = a_1\dot{x} + 3a_2(x - x_e)^2\dot{x} \\ \ddot{f}_e = a_1\ddot{x} + 3a_2(x - x_e)^2\ddot{x} + 6a_2(x - x_e)\dot{x}^2 \end{cases} \quad (15)$$

where $a_1 = 10^2 m \omega_0^2$, $a_2 = 10^6 m \frac{3\beta_0^2 \epsilon}{4}$.

In free space, the end-effector does not exert force on the flexible environment, the constant impedance controller is designed to track the desired position. In contact space, the variable impedance controller is used to track the force of the manipulator in the force direction. For convenience, this paper takes one-dimensional force in the vertical direction for example, the impedance relation can be written as,

$$\begin{cases} m_d \ddot{e} + b_d \dot{e} + k_d e = 0 & (\text{in free space}) \\ (m_d + \Delta m_d(t)) \ddot{e}(t) + (b_d + \Delta b_d(t)) \dot{e}(t) + (k_d + \Delta k_d(t)) e(t) = \Delta f(t) & (\text{in contact space}) \end{cases} \quad (16)$$

where $e = x_d - x$, $\Delta f = f_e - f_d$, $\Delta m_d(t)$, $\Delta b_d(t)$ and $\Delta k_d(t)$ are time-varying to minimize the force tracking error Δf . The adaptation are defined as,

$$\begin{cases} \Delta m_d(t) = \frac{\Delta f(t)}{\ddot{e}(t)} + \frac{m_d}{g(x,t)\ddot{e}(t)} [-6a_2(x(t) - x_e)\dot{x}^2(t) + 2\dot{g}(x,t)\dot{x}_d(t) + \ddot{g}(x,t)x_d(t)] \\ \Delta b_d(t) = b_d \frac{\dot{g}(x,t)x_d(t)}{g(x,t)\dot{e}(t)} \\ \Delta k_d(t) = k_d \left[\frac{x(t)}{g(x,t)e(t)} - \frac{f_d(t)}{g(x,t)e(t)} - \frac{\Delta f(t)}{g(x,t)e(t)} + \frac{\Phi(t)}{g(x,t)e(t)} \right] \\ \Phi(t) = \Phi(t - \lambda) - \alpha \Delta f(t - \lambda) \\ g(x,t) = a_1 + 3a_2[x(t) - x_e]^2 \end{cases} \quad (17)$$

where λ represents the sampling time of the controller, α denotes a positive constant. The reference trajectory is expressed as follows,

$$\begin{cases} \ddot{X}_r(t) = \ddot{X}_d(t) - \frac{1}{M_d(t)} [\Delta F(t) - B_d(t)(\dot{X}_r(t-1) - \dot{X}_d(t)) - k_d(t)(X_r(t-1) - X_d(t))] \\ \dot{X}_r(t) = \dot{X}_r(t-1) + \dot{X}_r(t)\lambda \\ X_r(t) = X_r(t-1) + \dot{X}_r(t)\lambda \end{cases} \quad (18)$$

where X_r represents the reference trajectory.

According to Eq. (15), substituting Eq. (17) into Eq. (16), yields,

$$\begin{aligned} \Delta f(t) &= [m_d + \Delta m_d(t)] \ddot{e}(t) + [b_d + \Delta b_d(t)] \dot{e}(t) + [k_d + \Delta k_d(t)] e(t) \\ &= m_d [\ddot{x}_d(t) - \frac{\ddot{f}_e(t)}{g(x,t)} + \frac{2\dot{g}(x,t)\dot{x}_d(t) + \ddot{g}(x,t)x_d(t)}{g(x,t)}] + \Delta f(t) + b_d [\dot{x}_d(t) - \frac{\dot{f}_e(t)}{g(x,t)} \\ &\quad + \frac{\dot{g}(x,t)x_d(t)}{g(x,t)\dot{e}(t)}] + k_d [x_d(t) - \frac{f_d(t)}{g(x,t)}] + k_d \frac{\Phi(t - \lambda)}{g(x,t)} - k_d \alpha \frac{\Delta f(t - \lambda)}{g(x,t)} - k_d \frac{\Delta f(t)}{g(x,t)} \end{aligned} \quad (19)$$

Simplifying and multiplying both sides of Eq (19) by $g(x,t)$, we obtain,

$$\begin{aligned} & m_d [g(x,t)\ddot{x}_d(t) + 2\dot{g}(x,t)x_d(t) + \ddot{g}(x,t)x_d(t) - \ddot{f}_e(t)] \\ & + b_d [g(x,t)\dot{x}_d(t) - \dot{f}_e(t) + \dot{g}(x,t)x_d(t)] + k_d [g(x,t)x_d(t) - f_d(t)] \\ & = m_d \Delta \ddot{f}(t) + b_d \Delta \dot{f}(t) + k_d \Delta f(t) + k_d \alpha \Delta f(t - \lambda) - k_d \Phi(t - \lambda) \end{aligned} \quad (20)$$

Defining $c(t) = \Delta f$ and $r(t) = g(x,t)x_d - f_d$, Eq. (20) can be rewritten as,

$$m_d \ddot{r} + b_d \dot{r} + k_d r = m_d \ddot{c} + b_d \dot{c} + k_d c - k_d \Phi(t - \lambda) + \alpha k_d c(t - \lambda) \quad (21)$$

Basing on the principle of dispersion, n elements of Φ series can be expanded as,

$$k_d \Phi(t - \lambda) = k_d (\Phi(t - (n+1)\lambda) - \alpha c(t - (n+1)\lambda) - \dots - \alpha c(t - 2\lambda)) \quad (22)$$

The initial value of $\Phi(t - (n+1)\lambda)$ is generally set to 0, Eq. (21) can be rewritten as,

$$m_d \ddot{r} + b_d \dot{r} + k_d r = m_d \ddot{c} + b_d \dot{c} + k_d c + k_d (\alpha c(t - (n+1)\lambda) + \dots + \alpha c(t - 2\lambda) + \alpha c(t - \lambda)) \quad (23)$$

According to the Laplace transform, the transfer function is:

$$\frac{c(s)}{r(s)} = \frac{m_d s^2 + b_d s}{T(s)} \quad (24)$$

where $T(s) = m_d s^2 + b_d s + k_d + k_d(\alpha(e^{-(n+1)\lambda s} + \dots + e^{-\lambda s}))$.

The characteristic equation of the system is follows,

$$m_d s^2 + b_d s + k_d + k_d \alpha (e^{-(n+1)\lambda s} + \dots + e^{-\lambda s}) = 0 \quad (25)$$

Assuming that n is a large enough number, we have $\sum_{n=1}^{\infty} e^{-\lambda n s} = \frac{e^{-\lambda s}}{1 - e^{-\lambda s}}$.

Then, the characteristic equation can be expanded by Taylor series when the sampling rate is sufficient,

$$\lambda m_d s^3 + \lambda b_d s^2 + \lambda k_d (1 - \alpha) s + k_d \alpha = 0 \quad (26)$$

The stability conditions of the system can be obtained according to Routh stability criterion yield,

$$0 < \alpha < \frac{\lambda b_d}{\lambda b_d + m_d} \quad (27)$$

So when the input is a step function and can be denoted as $r(s) = 1/s$, the steady-state error in the frequency domain is as follows,

$$e_{ss} = \lim_{s \rightarrow 0} sE(s) = \lim_{s \rightarrow 0} s(c(s) - r(s)) = -1 \quad (28)$$

Considering the Eq. (28), the following conclusion can be obtained,

$$\lim_{s \rightarrow 0} sc(s) = 0, \lim_{t \rightarrow 0} c(t) = 0 \quad (29)$$

Therefore, when $t \rightarrow \infty$, we have $\Delta f \rightarrow 0$. The error between actual contact force and expected contact force converges to zero.

Different from most adaptive variable impedance trajectory generators, this paper proposes a *PBAVITG* based on Eq. (5). The impedance parameters can be updated adaptively to reduce the force tracking error by the force and position feedback on the premise of ensuring the stability of *PBAVITG*.

3.2 Adaptive fuzzy-based controller design

Defining the position and velocity tracking errors of the manipulator,

$$E_s = X_r - x_1, \dot{E}_s = \dot{X}_r - \dot{x}_2 \quad (30)$$

where $x_1 = X$ and $x_2 = \dot{X}$.

Defining a composite error as follows,

$$s = \dot{E}_s + \Lambda e^* \quad (31)$$

where $\Lambda = \Lambda^T$ represents a diagonal positive definite matrix, and e^* is expressed as follows,

$$e^* = \begin{cases} E_s & (\text{in free space}) \\ \Delta F & (\text{in contact space}) \end{cases} \quad (32)$$

Differentiating Eq. (31) and multiplying $M_0(x_1)$ on both sides, we can obtain,

$$\begin{aligned}
M_{0x}\dot{s} &= M_{0x}(\ddot{E}_s + \wedge \dot{e}^*) \\
&= M_{0x}(\ddot{X}_r + \wedge \dot{e}^*) - M_{0x}\dot{x}_2 \\
&= M_{0x}(\ddot{X}_r + \wedge \dot{e}^*) - (F - F_e - F_{\tau_d} - Y_x - C_{0x}x_2 - G_{0x}) \\
&= F_e + F_{\tau_d} - F - C_{0x}s + \Psi(x_1, x_2, e^*)
\end{aligned} \tag{33}$$

where $\Psi(x_1, x_2, e^*)$ is an unknown nonlinear function and defined as follows,

$$\Psi(x_1, x_2, e^*) = M_{0x}(\ddot{X}_r + \wedge \dot{e}^*) + G_{0x} + C_{0x}(\dot{x}_r + \wedge e^*) + Y_x \tag{34}$$

In this section, we use *FLS* to approximate the uncertain nonlinear function, i.e.

$$\Psi(x_1, x_2, e^*) = \Theta^{*T}\xi(x_1, x_2, e^*) + \varepsilon(x_1, x_2, e^*) \tag{35}$$

where the definitions of Θ^{*T} , $\xi(x_1, x_2, e^*)$ and $\varepsilon(x_1, x_2, e^*)$ are shown in the Eq. (3). According to the above derivation, variable impedance control law based on *FLS* can be designed as,

$$\tau = J^T[k_s s + F_e + \hat{\Theta}^T\xi(x_1, x_2, e^*) + u] \tag{36}$$

where $k_s > 0$ is the controller gain, u is a robust term, which can be used to compensate the external disturbance and approximation error of *FLS*.

Substituting Eq. (36) into (33), the system error can be expressed as follows,

$$M_{0x}\dot{s} = F_{\tau_d} - C_{0x}s - (k_s s + \hat{\Theta}^T\xi(x_1, x_2, e^*) + u) + \Psi(x_1, x_2, e^*) \tag{37}$$

Since $\Psi(x_1, x_2, e^*) - \hat{\Theta}^T\xi(x_1, x_2, e^*) = \Theta^{*T}\xi(x_1, x_2, e^*) + \varepsilon(x_1, x_2, e^*) - \hat{\Theta}^T\xi(x_1, x_2, e^*) = \tilde{\Theta}^T\xi(x_1, x_2, e^*) + \varepsilon(x_1, x_2, e^*)$, and $\tilde{\Theta} = \Theta^* - \hat{\Theta}$ represents the weight estimated error.

Assumption 2 *The reconstruction error of FLS is bounded and satisfy,*

$$\|\varepsilon(x_1, x_2, e^*)\| \leq \rho_\varepsilon \tag{38}$$

where ρ_ε is the positive constants.

Then, according to Assumptions 1 and 2, the minimum reconstruction error of *FLS* and the external disturbance are bounded as,

$$\|\varepsilon(x_1, x_2, e^*) + \tau_d\| \leq \rho_\varepsilon + \tau_D \triangleq \varpi_0 \tag{39}$$

where ϖ_0 is a positive constant.

3.3 Stability analysis

Theorem 1 *Basing on the robot dynamics Eq. (13), and supposing that Assumptions 1 and 2 are satisfied, the fuzzy-based adaptive impedance control law can be designed as Eq. (36), where the robust compensation term can be expressed as,*

$$u = \varpi_0 \text{sgn}(s) \tag{40}$$

The *FLS* adaptive law is:

$$\dot{\hat{\Theta}} = \Gamma[\xi(x_1, x_2, e^*)s - \eta\hat{\Theta}] \quad (41)$$

where Γ and η are positive constants. Then, the adaptive fuzzy-based controller proposed as Eq. (36) is stable, the composite error s and the weight estimation error $\hat{\Theta}$ are uniformly ultimately bounded. It means that the position trajectory tracking error e in free space and the force tracking error Δf in contact space are bounded and can be made as small as possible.

Proof

Choosing a Lyapunov function candidate as,

$$V = \frac{1}{2}s^T M_{0x}s + \frac{1}{2}\text{tr} \left\{ \tilde{\Theta}^T \Gamma^{-1} \tilde{\Theta} \right\} \quad (42)$$

Differentiating the above Lyapunov function and substituting Eq. (42). According to Property 2, we have,

$$\begin{aligned} \dot{V} &= s^T M_{0x}\dot{s} + \frac{1}{2}s^T \dot{M}_{0x}s + \text{tr} \left\{ \tilde{\Theta}^T \Gamma^{-1} \dot{\tilde{\Theta}} \right\} \\ &= s^T [F_{\tau_d} - k_s s - C_{0x}s - u + \tilde{\Theta}^T \xi(x_1, x_2, e^*) + \varepsilon(x_1, x_2, e^*)] + \frac{1}{2}s^T \dot{M}_{0x}s + \text{tr} \left\{ \tilde{\Theta}^T \Gamma^{-1} \dot{\tilde{\Theta}} \right\} \\ &= s^T [F_{\tau_d} - k_s s - u + \tilde{\Theta}^T \xi(x_1, x_2, e^*) + \varepsilon(x_1, x_2, e^*)] + \text{tr} \left\{ \tilde{\Theta}^T \Gamma^{-1} \dot{\tilde{\Theta}} \right\} \end{aligned} \quad (43)$$

Considering Eq. (40), we can obtain,

$$s^T [F_{\tau_d} - u + \varepsilon(x_1, x_2, e^*)] \leq 0 \quad (44)$$

According to the updating law Eq. (41), we can obtain,

$$s^T \tilde{\Theta}^T \xi(x_1, x_2, e^*) + \text{tr} \left\{ \tilde{\Theta}^T \Gamma^{-1} \dot{\tilde{\Theta}} \right\} = \eta \text{tr} \left\{ \tilde{\Theta}^T \dot{\tilde{\Theta}} \right\} \quad (45)$$

Therefore, Eq. (43) is bounded as,

$$\dot{V} \leq -s^T k_s s + \eta \text{tr} \left\{ \tilde{\Theta}^T \dot{\tilde{\Theta}} \right\} \leq -s^T k_s s - \frac{\eta}{2} \text{tr} \left\{ \tilde{\Theta}^T \tilde{\Theta} \right\} + \frac{\eta}{2} \text{tr} \left\{ \Theta^{*T} \Theta^* \right\} \quad (46)$$

The above Eq. (46) can be rewritten as,

$$\dot{V} \leq -\epsilon V + \gamma \quad (47)$$

where $\epsilon = \frac{\min(\lambda_{\min}(k_s), \eta/2)}{\max(\lambda_{\max}(M_{0x}), \lambda_{\max}(\Gamma^{-1}))}$ and $\frac{\eta}{2} \text{tr} \left\{ \Theta^{*T} \Theta^* \right\} \leq \gamma$, γ is a positive constant.

Based on Lyapunov stability theorem, the closed-loop system is stable. And solving the inequality Eq. (47) yields,

$$0 \leq V(t) \leq [V(t_0) - \frac{\gamma}{\epsilon}]e^{-\epsilon t} + \frac{\gamma}{\epsilon} \quad (48)$$

where t_0 is the initial time. Eq. (48) means that the error signals s and $\tilde{\Theta}$ are uniformly ultimately bounded. Moreover, for arbitrary $s(t_0)$, as long as $t > t_0$, we have,

$$\|s\| \leq \sqrt{\frac{V(t_0) - \gamma/\epsilon}{\min(\lambda_{\min}(M_{0x}), \lambda_{\min}(\Gamma))}} \|s(t_0)\|^2 e^{-\epsilon t} + \frac{2\gamma}{\min(\lambda_{\min}(M_{0x}), \lambda_{\min}(\Gamma))\epsilon} \quad (49)$$

Since the first term within the square root in Eq. (49) will converges to zero, it means that the composite error $\|s\| \leq \sqrt{2\gamma/\min(\lambda_{\min}(M_{0x}), \lambda_{\min}(\Gamma))\epsilon}$ as $t \rightarrow +\infty$. Therefore, when the parameters are properly selected, the composite error can be minimized, and the position tracking error e in the free space and the force tracking error Δf in the contact space are bounded.

According to the above analysis, the control structure of the system can be shown in Fig. 2.

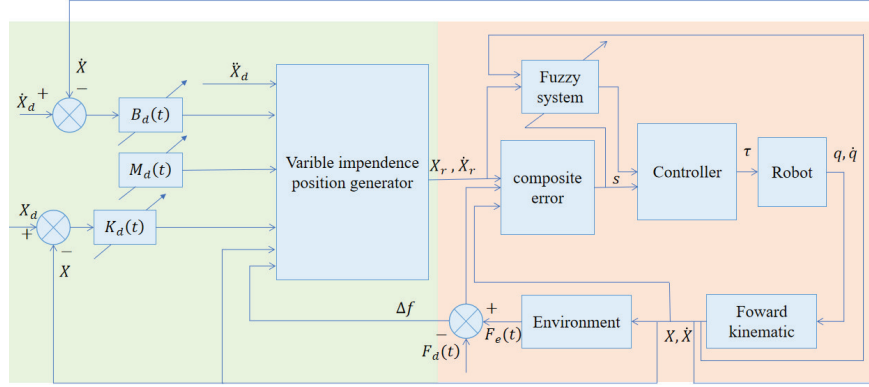


Fig. 2: The fuzzy-based variable impedance control schematic

4 Simulation studies

To verify the above method, simulations are conducted on a two-link manipulator, which is described as,

$$M(q) = \begin{bmatrix} m_1 l_1^2 + m_2(l_2^2 + l_2^2 + 2m_2 + l_1 l_2 c_2) & m_2 l_2^2 + m_2 l_1 l_2 c_2 \\ m_2 l_2^2 + m_2 l_1 l_2 c_2 & m_2 l_2^2 \end{bmatrix} \quad (50)$$

$$C(q) = \begin{bmatrix} -2m_2 l_1 l_2 \dot{q}_2 s_2 & m_2 l_1 l_2 \dot{q}_2 s_2 \\ m_2 l_1 l_2 \dot{q}_2 s_2 & 0 \end{bmatrix} \quad (51)$$

$$G(q) = \begin{bmatrix} (m_1 + m_2) l_1 g c_1 + m_2 l_2 g c_{12} \\ m_2 l_2 g c_{12} \end{bmatrix} \quad (52)$$

where the mass of link 1 and link 2 are denoted as m_1 and m_2 , respectively; The length of link 1 and link 2 are denoted as l_1 and l_2 , respectively; $\sin(q_i)$, $\cos(q_i)$, and c_{ij} can be shortened to s_i , c_i and c_{ij} , respectively, for $i = 1, 2$ and $j = 1, 2$, g is the acceleration of gravity.

4.1 Design procedure

To verify the proposed method in Section. 3, the step-by-step procedures of the *FBAVIC* are outlined as follows:

Step 1 Construct *PBAVITG*: Select the appropriate impedance parameters, $m_d = 1$, $b_d = 50$, $k_d = 500$ in free space. $m_d = 1$, $b_d = 1$, $k_d = 1$, $\alpha = 0.0009$ in contact space.

Step 2 Construct the *FLS*: Set the inputs are $x = [x_1^T, x_2^T, \Lambda e^{*T}]^T$, choose 5 Gaussian relationship functions as,

$$\mu_{A_i}^l(x_i) = \exp \left\{ - \frac{x_i + \pi/6 - (l-1)\pi/12}{\pi/24} \right\}^2$$

where $i = 1, 2, 3$, $l = 1, 2, 3, 4, 5$, and select the learning parameter as $\Gamma = 100$ in Eq. (41).

Step 3 Construct the *FBAVIC*: Choose controller gain $K_s = 500I_{2 \times 2}$ and set $\varpi_0 = 2I_{2 \times 2}$ in Eq. (40). $\Lambda = 2I_{2 \times 2}$ in free space and $\Lambda = 0.1I_{2 \times 2}$ in contact space in Eq. (31). The adaptive variable impedance controller based on *FLS* can be obtained from Theorem 1.

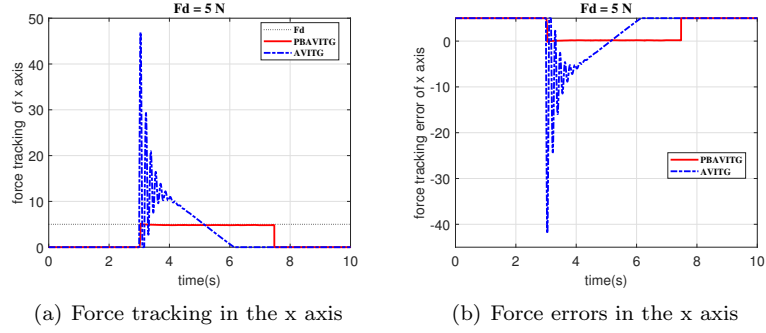


Fig. 3: Force tracking and errors of PBAVITG and AVITG

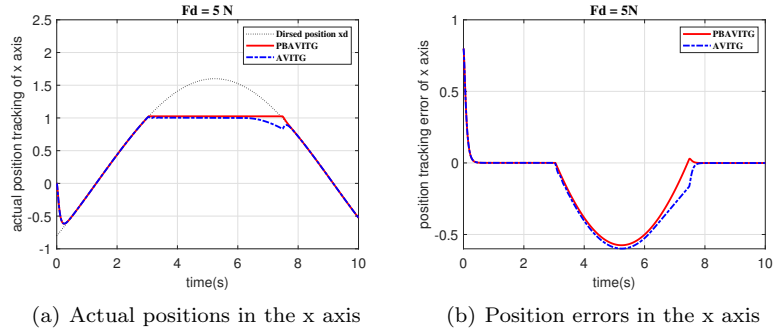


Fig. 4: Actual position and errors of PBAVITG and AVITG in the x axis

4.2 Simulation results

In the subsection, two examples are conducted on a two-link manipulator. The nominal parameters of robot are chosen as $m_1 = 0.8$ kg, $m_2 = 0.9$ kg, $l_1 = 1.1$ m, $l_2 = 0.9$ m and $g = 9.8$ m/s², while the actual parameters of robot are $m_1 = m_2 = 1$ kg and $l_1 = l_2 = 1$ m to introduce the parameters uncertainties. Choosing the contact force Eq. (5) in the x direction, where $\omega_0 = 0.2$ and $\beta_0^2 \epsilon = 0.4$, the parameters were selected according to the literature [9]. And the desired position trajectory is $X_d(t) = [1.6 \sin(0.4t + \pi/6), 1.6 \sin(0.4t + \pi/3)]^T$ m. To testing the robustness of this proposed method, choosing external disturbance as $\tau_d = [-2 \cos(2t), 2 \sin(2t)]^T$ N/m.

4.2.1 Example 1

Assuming that the desired force $F_d = [5, 0]^T$ N is exerted on the manipulator as $x \geq x_e \geq 1$ m in x direction. To test the superiority of the force contact environmental model and the proposed *PBAVITG*, the adaptive variable impedance trajectory generator (*AVITG*) [38] is compared with the proposed method. In the *AVITG*, only the damping coefficient adaptively changed by the force feedback error, and the traditional spring environmental model is used. Fig.3(a) and (b) show the force tracking results and errors for invariable force. Figs.4(b) and 5(b) show the desired position tracking errors between desired and actual positions of end-effector in the direction x and y of Cartesian space, respectively.

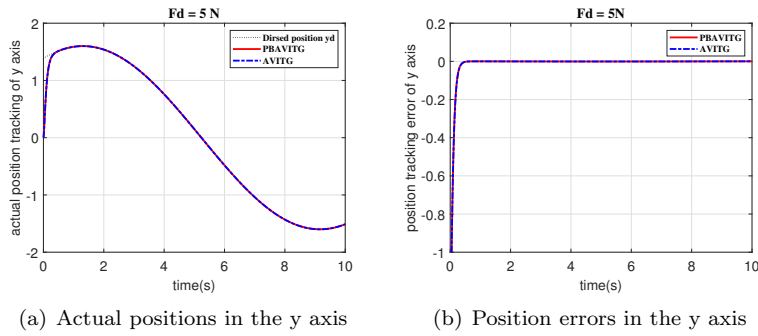


Fig. 5: Actual position and errors of PBAVITG and AVITG in the y axis

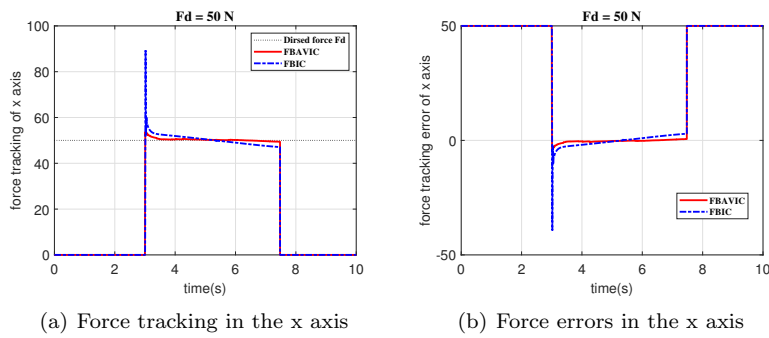


Fig. 6: Force tracking and errors of FBAVIC and FBIC

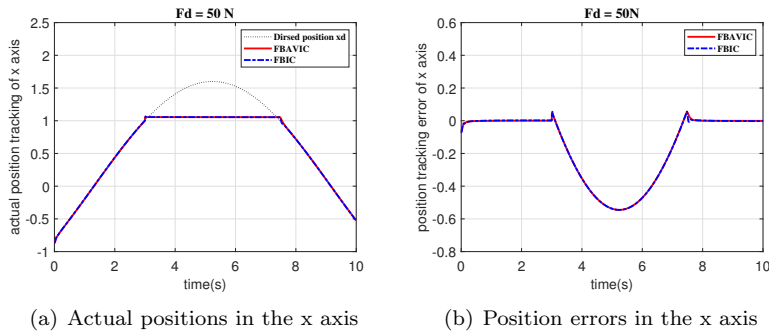


Fig. 7: Actual position and errors of PBAVITG and AVITG in the x axis

From Fig.3, it can be found that the proposed *PBAVITG* has less error and less overshoot in the initial stage of force tracking compared with *AVITG*. Moreover, The oscillation time in *AVITG* is longer. And from Fig.4(a), it can be seen that the proposed *PBAVITG* has a more smooth trajectory in the direction x of Cartesian space, the generated trajectory of *AVITG* in the force direction is unable to track the desired force. The reason is that the model adopted in *PBAVITG* is derived from a nonlinear spring damp-restorer model, and added a nonlinear recovery term compared with the spring model adopted in *AVITG*. So when the manipulator is transforming from the free space to contact space, the overshoot of *PBAVITG* is smaller

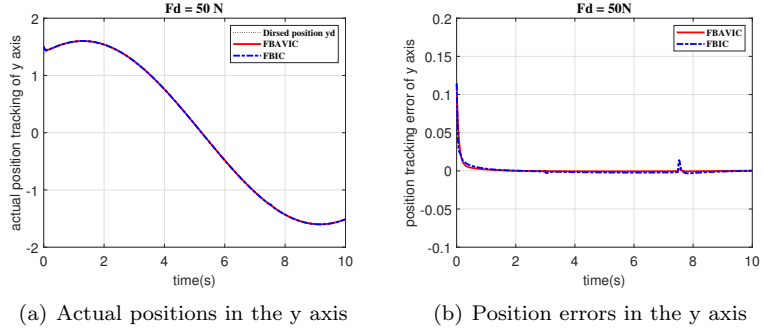


Fig. 8: Actual position and errors of PBAVITG and AVITG in the y axis

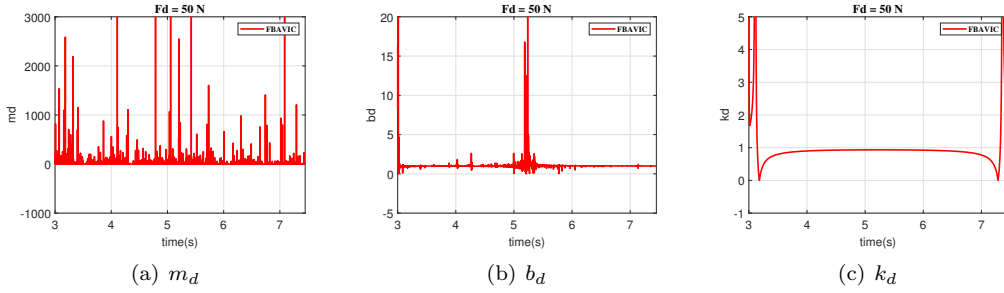


Fig. 9: Adaptive impedance parameter variation diagram

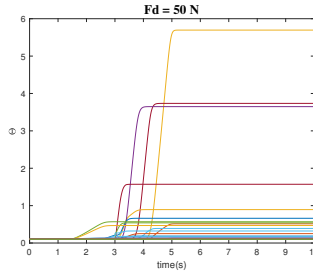


Fig. 10: Adaptive adjustment parameters of FLS

than that of *AVITG*, and the oscillation time of *PBAVITG* is shorter than that of *AVITG* in the initial stage of force tracking. From Fig.5, it can be seen that the two methods have good track tracking performance in the direction y of Cartesian space. Although *AVITG* can obtain a smooth trajectory and have a good control performance in the case of direct contact with the environmental model, it is not applicable in the case of spatial transformation in this experiment. The reason is that the transformation of space and the nonlinear contact force put forward higher requirements for the adaptability of the control method. Moreover, the behavior of the contact environment is only expressed by the stiffness coefficient, which is not only not enough, but also too stiff in the conversion process, which is prone to produce larger overshoot and long-term oscillation at the instant of contact. Therefore, the above results indicate that the performance

of *PBAVITG* is better than that of *AVITG*, the superiority of the novel force contact-based environmental model and the adaptability of the variable impedance control method are proved.

4.2.2 Example 2

The desired force $F_d = [50, 0]^T$ N is exerted on the end-effector to verify the performance of the proposed *FBAVIC*. The two groups of methods adopt the nonlinear environmental model mentioned in this paper, but the control methods are different. The proposed *FBAVIC* and fuzzy-based impedance control (*FBIC*) are compared for specific flexible environmental models considering the uncertainty and disturbance of manipulator. In this experiment, Fig.6(a) and (b) show the force tracking results and errors of *FBAVIC* and *FBIC*. Figs.7(a) and 8(a) show the results of tracking the desired trajectory by two methods in the direction x and y of Cartesian space, respectively. Figs.7(b) and 8(b) show the position tracking errors between the desired and actual trajectories in the direction x and y of Cartesian space, respectively. Fig.9 shows the variation of adaptive impedance parameters in contact space. Fig.10 shows the update rate of adaptive adjustment parameters of *FLS*.

From Fig.6, it can be found that the overshoot and the force tracking error of the proposed *FBAVIC* are greatly reduced in comparison to *FBIC*. The reason is that the impedance parameters in the *FBAVIC* are updating adaptively. Compared with the *FBIC*, the adaptability of the proposed *FBAVIC* is stronger than that of *FBIC* due to the real-time feedback of force error in the process of force tracking, so the force tracking performance of the proposed *FBAVIC* is better than that of *FBIC*. From Figs.7-8, it can be seen that the position tracking performance of the proposed *FBAVIC* is similar to that of *FBIC*. From Fig.9, it can be concluded that the adaptive impedance parameters change irregularly, which is determined by the adaptive law. Fig.10 shows that the adaptive adjustment parameters of *FLS* are bounded and can be converged to the optimal values in finite time.

According to the above analysis, it can be concluded that the proposed *FBAVIC* not only reduce the force overshoot and oscillation during contact, but also make the force tracking error smaller than *FBIC*, which meets the design requirements and improves the adaptability and robustness of the system.

5 Conclusion

In this paper, a fuzzy-based adaptive variable impedance control is proposed for the robotic system in flexible environment. In this control scheme, according to the nonlinear force contact-based environmental model, an adaptive fuzzy variable impedance controller is designed to track the desired contact force trajectory of the manipulator. And the impedance parameters of the variable impedance control are adjusted adaptively according to force feedback. The boundness of force/position tracking errors and the stability of the controller are proved by Routh stability criterion and Lyapunov stability theory, and the *FLS* is used to compensate for the uncertainties of the system dynamics parameters. Finally, the feasibility and effectiveness of the control strategy are verified by simulation on a two-link manipulator.

6 Statements and Declarations

6.1 Funding

This work was supported by the National Natural Science Foundation of China (62273311, 61773351, 61733004), the Program for Science & Technology Innovation Talents in Universities of Henan Province (20HASTIT031), and the Key Specialized Research and Development Breakthrough in Henan Province (222102220117).

6.2 Competing Interests

The authors have no relevant financial or non-financial interests to disclose.

6.3 Author Contributions

All authors contributed to the study conception and design. Material preparation, data collection and analysis were performed by Jinzhu Peng, Ying Guo and Shuai Ding. The first draft of the manuscript was written by Jinzhu Peng and Ying Guo and all authors commented on previous versions of the manuscript. All authors read and approved the final manuscript.

6.4 Data Availability

The datasets are available from the corresponding author on reasonable request.

References

1. L. D. Evjemo, T. Gjerstad, E. I. Grøtli, and G. Sziebig, "Trends in smart manufacturing: Role of humans and industrial robots in smart factories," *Current Robotics Reports*, vol. 1, no. 2, pp. 35–41, 2020.
2. Z. Li, S. Li, and X. Luo, "An overview of calibration technology of industrial robots," *IEEE/CAA Journal of Automatica Sinica*, vol. 8, no. 1, pp. 23–36, 2021.
3. K. K. Babarahmati, C. Tiseo, J. Smith, H.-C. Lin, M. S. Erden, and M. Mistry, "Fractal impedance for passive controllers: a framework for interaction robotics," *Nonlinear Dynamics*, pp. 1–17, 2022.
4. M. Schumacher, J. Wojtusch, P. Beckerle, and O. von Stryk, "An introductory review of active compliant control," *Robotics and Autonomous Systems*, vol. 119, pp. 185–200, 2019.
5. H.-Y. Li, I. Paranawithana, L. Yang, T. S. K. Lim, S. Foong, F. C. Ng, and U.-X. Tan, "Stable and compliant motion of physical human–robot interaction coupled with a moving environment using variable admittance and adaptive control," *IEEE Robotics and Automation Letters*, vol. 3, no. 3, pp. 2493–2500, 2018.
6. J. Hu, H. Lai, Z. Chen, X. Ma, and B. Yao, "Desired compensation adaptive robust repetitive control of a multi-dofs industrial robot," *ISA transactions*, 2021. doi:<https://doi.org/10.1016/j.isatra.2021.10.002>.
7. P. Gierlak and M. Szuster, "Adaptive position/force control for robot manipulator in contact with a flexible environment," *Robotics and Autonomous Systems*, vol. 95, pp. 80–101, 2017.
8. L. Baptista, J. Sousa, and J. S. da Costa, *Predictive force control of robot manipulators in nonrigid environments*. Citeseer, 2006.
9. Q. Luo and J. Xiao, "Contact and deformation modeling for interactive environments," *IEEE Transactions on Robotics*, vol. 23, no. 3, pp. 416–430, 2007.
10. M. N. Omar and Y. Zhong, "Flexible mass spring method for modelling soft tissue deformation," *International Journal of Engineering Technology and Sciences*, vol. 7, no. 2, pp. 24–41, 2020.
11. N. Hogan, "Impedance control: An approach to manipulation," in *1984 American control conference*, pp. 304–313, IEEE, 1984.
12. M. Reibert, "Hybrid position/force control of manipulators," *ASME, Journal of Dynamic Systems, Measurement, and Control*, vol. 103, pp. 2–12, 1981.

13. H. Wang, J. Peng, F. Zhang, H. Zhang, and Y. Wang, "High-order control barrier functions-based impedance control of a robotic manipulator with time-varying output constraints," *ISA transactions*, 2022. doi:<https://doi.org/10.1016/j.isatra.2022.02.013>.
14. G. Nazmara, M. M. Fateh, and S. M. Ahmadi, "A robust adaptive impedance control of robots," in *2018 6th RSI International Conference on Robotics and Mechatronics (IcRoM)*, pp. 40–45, IEEE, 2018.
15. C. Saldarriaga, N. Chakraborty, and I. Kao, "Damping selection for cartesian impedance control with dynamic response modulation," *IEEE Transactions on Robotics*, vol. 38, no. 3, pp. 1915–1924, 2021.
16. S. H. Kang, M. Jin, and P. H. Chang, "A solution to the accuracy/robustness dilemma in impedance control," *IEEE/ASME Transactions on Mechatronics*, vol. 14, no. 3, pp. 282–294, 2009.
17. M. M. Fateh and R. Babaghasabha, "Impedance control of robots using voltage control strategy," *Nonlinear Dynamics*, vol. 74, no. 1, pp. 277–286, 2013.
18. A. Albu-Schaffer and G. Hirzinger, "Cartesian impedance control techniques for torque controlled light-weight robots," in *Proceedings 2002 IEEE International Conference on Robotics and Automation*, vol. 1, pp. 657–663, IEEE, 2002.
19. G. Chen, S. Guo, B. Hou, J. Wang, and X. Wang, "Fractional order impedance control," in *Nonlinear Dynamics and Control*, vol. 2, pp. 167–175, Springer, 2020.
20. A. Izadbakhsh, S. Khorashadizadeh, and S. Ghandali, "Robust adaptive impedance control of robot manipulators using szász–mirakyan operator as universal approximator," *ISA transactions*, vol. 106, pp. 1–11, 2020.
21. V. Khoshdel, A. Akbarzadeh, N. Naghavi, A. Sharifnezhad, and M. Souzanchi-Kashani, "semg-based impedance control for lower-limb rehabilitation robot," *Intelligent Service Robotics*, vol. 11, no. 1, pp. 97–108, 2018.
22. P. Li, S. S. Ge, and C. Wang, "Impedance control for human-robot interaction with an adaptive fuzzy approach," in *2017 29th Chinese Control and Decision Conference (CCDC)*, pp. 5889–5894, IEEE, 2017.
23. Z. Yang, J. Peng, and Y. Liu, "Adaptive neural network force tracking impedance control for uncertain robotic manipulator based on nonlinear velocity observer," *Neurocomputing*, vol. 331, pp. 263–280, 2019.
24. S. Ding, J. Peng, H. Zhang, and Y. Wang, "Neural network-based adaptive hybrid impedance control for electrically driven flexible-joint robotic manipulators with input saturation," *Neurocomputing*, vol. 458, pp. 99–111, 2021.
25. J. Peng, S. Ding, Z. Yang, and J. Xin, "Adaptive neural impedance control for electrically driven robotic systems based on a neuro-adaptive observer," *Nonlinear Dynamics*, vol. 100, no. 2, pp. 1359–1378, 2020.
26. W. He, Y. Dong, and C. Sun, "Adaptive neural impedance control of a robotic manipulator with input saturation," *IEEE Transactions on Systems, Man, and Cybernetics: Systems*, vol. 46, no. 3, pp. 334–344, 2015.
27. W. He and Y. Dong, "Adaptive fuzzy neural network control for a constrained robot using impedance learning," *IEEE transactions on neural networks and learning systems*, vol. 29, no. 4, pp. 1174–1186, 2017.
28. T. Sun, L. Peng, L. Cheng, Z.-G. Hou, and Y. Pan, "Composite learning enhanced robot impedance control," *IEEE Transactions on Neural Networks and Learning Systems*, vol. 31, no. 3, pp. 1052–1059, 2019.
29. L. F. Baptista and J. M. S. da Costa, "A force control approach of robotic manipulators in non-rigid environments," in *1999 European Control Conference (ECC)*, pp. 2777–2782, IEEE, 1999.
30. A. Jafari, J.-H. Ryu, M. Rezaei, R. Monfaredi, A. Talebi, and S. S. Ghidary, "An adaptive hybrid force/motion control design for robot manipulators interacting in constrained motion with unknown non-rigid environments," in *IEEE ISR 2013*, pp. 1–5, IEEE, 2013.
31. W. JIANQING, L. ZHIWEI, M. Yamakita, and K. Ito, "Adaptive hybrid control of manipulators on uncertain flexible objects," *Advanced robotics*, vol. 10, no. 5, pp. 469–485, 1995.
32. S. Jung, T. C. Hsia, and R. G. Bonitz, "Force tracking impedance control of robot manipulators under unknown environment," *IEEE Transactions on Control Systems Technology*, vol. 12, no. 3, pp. 474–483, 2004.
33. K. Lee and M. Buss, "Force tracking impedance control with variable target stiffness," *IFAC Proceedings Volumes*, vol. 41, no. 2, pp. 6751–6756, 2008.
34. H. Hu and J. Cao, "Adaptive variable impedance control of dual-arm robots for slabstone installation," *ISA transactions*, 2021. doi:<https://doi.org/10.1016/j.isatra.2021.10.020>.
35. D. Jinjun, G. Yahui, C. Ming, and D. Xianzhong, "Symmetrical adaptive variable admittance control for position/force tracking of dual-arm cooperative manipulators with unknown trajectory deviations," *Robotics and Computer-Integrated Manufacturing*, vol. 57, pp. 357–369, 2019.
36. X. Zhang, T. Sun, and D. Deng, "Neural approximation-based adaptive variable impedance control of robots," *Transactions of the Institute of Measurement and Control*, vol. 42, no. 13, pp. 2589–2598, 2020.
37. K. Kronander and A. Billard, "Stability considerations for variable impedance control," *IEEE Transactions on Robotics*, vol. 32, no. 5, pp. 1298–1305, 2016.
38. J. Duan, Y. Gan, M. Chen, and X. Dai, "Adaptive variable impedance control for dynamic contact force tracking in uncertain environment," *Robotics and Autonomous Systems*, vol. 102, pp. 54–65, 2018.
39. L. Roveda and D. Piga, "Robust state dependent riccati equation variable impedance control for robotic force-tracking tasks," *International Journal of Intelligent Robotics and Applications*, vol. 4, no. 4, pp. 507–519, 2020.